Resonant Enhancement of Inelastic Light Scattering in Strongly Correlated Materials

A. M. Shvaika,[1] O. Vorobyov,[1] J. K. Freericks,[2] and T. P. Devereaux[3]

[1]*Institute for Condensed Matter Physics of the National Academy of Sciences of Ukraine, 1 Svientsitskii Street, 79011 Lviv, Ukraine*
[2]*Department of Physics, Georgetown University, Washington, D.C. 20057, USA*
[3]*Department of Physics, University of Waterloo, Ontario N2L 3GI, Canada*

(Received 4 November 2003; published 21 September 2004)

We use dynamical mean field theory to find an exact solution for inelastic light scattering in strongly correlated materials such as those near a quantum-critical metal-insulator transition. We evaluate the results for $\mathbf{q} = 0$ (Raman) scattering and find that resonant effects can be quite large, and yield a double resonance, a significant enhancement of nonresonant scattering peaks, a joint resonance of both peaks when the incident photon frequency is on the order of U, and the appearance of an isosbestic point in all symmetry channels for an intermediate range of incident photon frequencies.

DOI: 10.1103/PhysRevLett.93.137402 PACS numbers: 78.30.–j, 71.10.–w, 71.27.+a, 71.30.+h

Inelastic light scattering is a powerful tool to unravel the nature of elementary excitations in a wide variety of materials [1], ranging from Kondo insulators [2,3], to high-temperature superconductors [4,5], to colossal magnetoresistance materials [6]. Experimental efforts have been brought to bear on a variety of strongly correlated materials to examine the elementary excitations of insulators and metals and how they evolve as the correlations are made to change via doping, for example.

It is widely believed that by tuning the incident photon frequency, features of the nonresonant spectra can be magnified by orders of magnitude; that is, the resonance serves as a bootstrap to raise the intensity of the nonresonant signal. However, a full, consistent theory is lacking [7,8]. Nonresonant scattering is derivable from a two-particle correlation function which can be treated by a variety of techniques, yet the resonant and mixed contributions involve higher particle correlations and are difficult to treat theoretically due to multiple-particle vertex renormalizations. Most of the approaches to light scattering in insulators examine the Loudon-Fleury model [9] which is most appropriate for off-resonant conditions. In the strong-coupling regime, a perturbative approach has been used to illustrate a number of important features of electronic resonant scattering processes [8,10]. The nonresonant case has also been examined, and an exact solution for correlated systems (in large spatial dimensions) is available for both the Falicov-Kimball [11] and Hubbard [12] models.

For an electronic system with nearest-neighbor hopping, the interaction with a weak external transverse electromagnetic field $\boldsymbol{A}$ is described by [8]

$$H_{\rm int} = -\frac{e}{\hbar c}\boldsymbol{j}\cdot\boldsymbol{A} + \frac{e^2}{2\hbar^2 c^2}\sum_{\alpha\beta} A_\alpha \gamma_{\alpha\beta} A_\beta, \tag{1}$$

where

$$j_\alpha = \sum_{\boldsymbol{k}} v_\alpha(\boldsymbol{k}) c^\dagger_\sigma(\boldsymbol{k}+\boldsymbol{q}/2) c_\sigma(\boldsymbol{k}-\boldsymbol{q}/2), \tag{2}$$

is the current operator, $v_\alpha(\boldsymbol{k}) = \partial\varepsilon(\boldsymbol{k})/\partial k_\alpha$ is the Fermi velocity, and

$$\gamma_{\alpha\beta} = \sum_{\boldsymbol{k}} \frac{\partial^2\varepsilon(\boldsymbol{k})}{\partial k_\alpha \partial k_\beta} c^\dagger_\sigma(\boldsymbol{k}+\boldsymbol{q}/2) c_\sigma(\boldsymbol{k}-\boldsymbol{q}/2) \tag{3}$$

is the stress tensor operator. The inelastic light-scattering cross section becomes ($\Omega = \omega_i - \omega_f$, $\mathbf{q} = \mathbf{k_i} - \mathbf{k_f}$ is the transferred photon frequency and momentum, respectively): $R(\Omega) = R_N(\Omega) + R_M(\Omega) + R_R(\Omega)$, where the nonresonant contribution is

$$R_N(\Omega) = 2\pi g^2(\boldsymbol{k}_i) g^2(\boldsymbol{k}_f) \sum_{if} \frac{\exp(-\beta\varepsilon_i)}{Z} \tilde{\gamma}_{if}\tilde{\gamma}_{fi}\delta(\varepsilon_f - \varepsilon_i - \Omega), \tag{4}$$

the mixed contribution is

$$\begin{aligned} R_M(\Omega) = 2\pi g^2(\boldsymbol{k}_i) g^2(\boldsymbol{k}_f) \sum_{ifl} \frac{\exp(-\beta\varepsilon_i)}{Z} \\ \times\Bigg[\tilde{\gamma}_{if}\Bigg(\frac{j^{(f)}_{fl} j^{(i)}_{li}}{\varepsilon_l - \varepsilon_i - \omega_i + i0^+} + \frac{j^{(i)}_{fl} j^{(f)}_{li}}{\varepsilon_l - \varepsilon_i + \omega_f - i0^+}\Bigg) + \Bigg(\frac{j^{(i)}_{il} j^{(f)}_{lf}}{\varepsilon_l - \varepsilon_i - \omega_i - i0^+} + \frac{j^{(f)}_{il} j^{(i)}_{lf}}{\varepsilon_l - \varepsilon_i + \omega_f + i0^+}\Bigg)\tilde{\gamma}_{fi}\Bigg]\delta(\varepsilon_f - \varepsilon_i - \Omega), \end{aligned} \tag{5}$$

and the resonant contribution is

$$R_R(\Omega) = 2\pi g^2(\boldsymbol{k}_i) g^2(\boldsymbol{k}_f) \sum_{ifll'} \frac{\exp(-\beta\varepsilon_i)}{\mathcal{Z}} \times \left(\frac{j_{il}^{(i)} j_{lf}^{(f)}}{\varepsilon_l - \varepsilon_i - \omega_i - i0^+} + \frac{j_{il}^{(f)} j_{lf}^{(i)}}{\varepsilon_l - \varepsilon_i + \omega_f + i0^+} \right) \times \left(\frac{j_{fl'}^{(f)} j_{l'i}^{(i)}}{\varepsilon_{l'} - \varepsilon_i - \omega_i - i0^+} + \frac{j_{fl'}^{(i)} j_{l'i}^{(f)}}{\varepsilon_{l'} - \varepsilon_i + \omega_f - i0^+} \right) \times \delta(\varepsilon_f - \varepsilon_i - \Omega). \quad (6)$$

Here $\omega_{i(f)}$ and $\boldsymbol{k}_{i(f)}$ denote the energy and momentum of the initial (final) states of the photons, $\varepsilon_{i(f)}$ are the eigenvalues corresponding to the eigenstates that describe the "electronic matter", and $g(\boldsymbol{k}) = (hc^2/V\omega_{\boldsymbol{k}})^{1/2}$ is the "scattering strength" with $\omega_{\mathbf{k}} = c|\boldsymbol{k}|$. We have introduced the following symbols $\tilde{\gamma} = \sum_{\alpha\beta} e_\alpha^i \gamma_{\alpha\beta} e_\beta^f$ and $j^{(i),(f)} = \sum_\alpha e_\alpha^{i,f} j_\alpha$, with the notation $\mathcal{O}_{if} = \langle i|\mathcal{O}|f\rangle$ for the matrix elements of an operator $\mathcal{O}$, $\mathcal{Z}$ for the partition function, and $\mathbf{e}^{i,f}$ for the incident and scattered light polarization vectors, respectively. We concentrate on the light-scattering response function $\chi(\Omega)$, which is related to the cross section, but with a Bose statistical factor removed:

$$R(\Omega) = \frac{2\pi g^2(\boldsymbol{k}_i) g^2(\boldsymbol{k}_f)}{1 - \exp(-\beta\Omega)} \chi(\Omega). \quad (7)$$

Inelastic light scattering examines charge excitations of different symmetries by employing polarizers on both the incident and scattered light. The A_{1g} symmetry has the full symmetry of the lattice and is primarily measured by taking the initial and final polarizations to be $\mathbf{e}^i = \mathbf{e}^f = (1, 1, 1, \ldots)$. The B_{1g} symmetry involves crossed polarizers: $\mathbf{e}^i = (1, 1, 1, \ldots)$ and $\mathbf{e}^f = (-1, 1, -1, 1, \ldots)$; while the B_{2g} symmetry is rotated by 45°, with $\mathbf{e}^i = (1, 0, 1, 0, \ldots)$ and $\mathbf{e}^f = (0, 1, 0, 1, \ldots)$. For Raman ($\mathbf{q} = 0$) scattering, it is easy to show that for a system with only nearest-neighbor hopping and in the limit of large dimensions, the A_{1g} sector has contributions from nonresonant, mixed, and resonant scattering, the B_{1g} sector has contributions from nonresonant and resonant scattering only, and the B_{2g} sector is purely resonant [11]. A full analysis for all $\mathbf{q}$ will be presented elsewhere; we focus only on Raman scattering ($\mathbf{q} = 0$) here.

Normally the matrix elements defined in Eqs. (4)–(6) cannot be easily determined for a many-body system in the thermodynamic limit. Instead, the light-scattering cross section expressions must be evaluated by first considering the relevant multitime correlation functions on the imaginary time axis, then Fourier transforming to a Matsubara frequency representation, and finally making an analytic continuation from the imaginary to the real frequency axis. In the case of nonresonant scattering, the expressions to be analytically continued depend on only one frequency; for mixed scattering they depend on two frequencies, and for resonant scattering, they depend on three. The analytic continuation procedure for the mixed and resonant Raman scattering is complicated, because it requires a multistep procedure, where first the transferred frequency is continued to the real axis, then the individual initial and final frequencies are continued to the real axis. In addition to the analytic continuation, we also must evaluate the dressed multitime correlation functions. There are renormalizations associated with two-particle "ladderlike" summations for a number of the relevant diagrams, but the symmetry of the velocity operator, and of the relevant multiparticle vertex functions (which are local in the large-dimensional limit) imply that there are no parquetlike summations, nor are there any three-particle or four-particle vertex renormalizations [13]. Since the two-particle vertex function for the Falicov-Kimball model is already known [14], the full Raman scattering problem can be solved via a straightforward but tedious procedure. The final formulas are cumbersome and will be presented elsewhere.

The Falicov-Kimball model Hamiltonian satisfies [15]

$$H = -\frac{t^*}{2\sqrt{d}} \sum_{\langle ij \rangle} (c_i^\dagger c_j + c_j^\dagger c_i) + U \sum_i c_i^\dagger c_i w_i \quad (8)$$

where $c_i^\dagger$ (c_i) create (annihilate) a conduction electron at site i, w_i is a classical variable (representing the localized electron number at site i) that equals 0 or 1, t^* is a renormalized hopping matrix that is nonzero between nearest neighbors on a hypercubic lattice in d dimensions (and we take the limit $d \to \infty$ [16]), and U is the local screened Coulomb interaction between conduction and

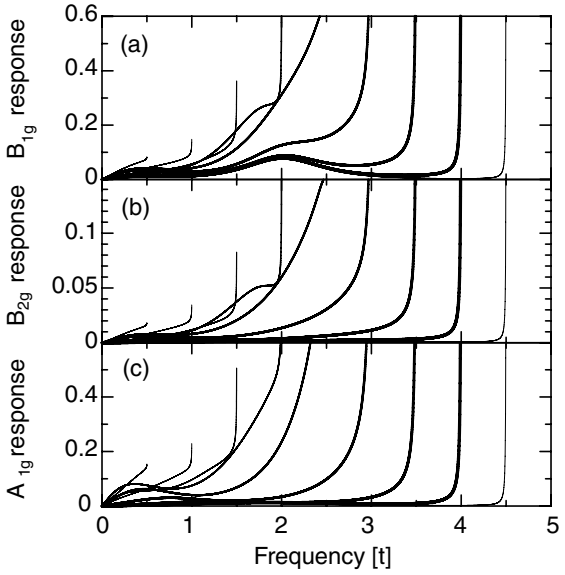

FIG. 1. Raman response function for different channels. We take $U = 2$, $T = 0.5$, and choose $\omega_i = 0.5 - 4.5$ in steps of 0.5 (the different line thicknesses correspond to different ω_i's).

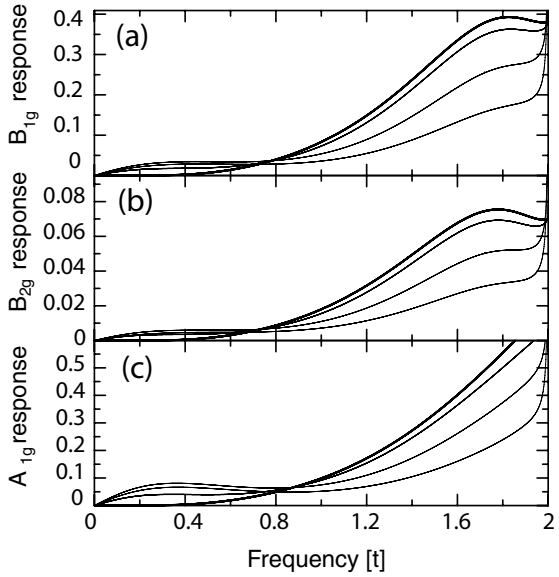

FIG. 2. Raman response function for $U = 2$ and $\omega_i = 2$ for different channels at $T = 1$, $T = 0.5$, $T = 0.2$, and $T = 0.05$. The temperature decreases as the lines are made thicker.

localized electrons. This model can be solved exactly by using dynamical mean field theory, as described by Brandt and Mielsch [17] and summarized in review articles [18].

We concentrate on the case with $U = 2$ here, which is just on the insulating side of the metal-insulator transition at half filling ($\rho_e = \langle w_i \rangle = 1/2$). This was the regime where the nonresonant response showed a number of interesting properties for both Raman [11] and inelastic x-ray scattering [19]. Since the nonresonant scattering has been shown to be model independent in the insulating phase [11,12], we conjecture that the qualitative results for mixed and resonant scattering are likewise model independent and hence are applicable to a wide range of different models and materials [20]. The Stokes Raman response function is plotted in Fig. 1 at $T = 0.5$ for nine different incident photon frequencies ω_i ranging from 0.5 to 4.5 in steps of 0.5. Since the transferred energy can be no larger than the incident photon energy, all scattering curves run from zero up to ω_i. The first thing to note in Fig. 1 is the large nearly vertical line that occurs as $\Omega \rightarrow \omega_i$. This is the so-called double resonance, which yields a strong enhancement to the Raman scattering when the energy of the scattered photon approaches zero (it is similar in many respects to the triple resonance [10], but the triple resonance requires an extra divergence in the renormalized vertex which does not occur in this model). In the Loudon-Fleury regime ($\omega_i \gg t^*, U$) [9], we see that the full response is essentially that of the unenhanced nonresonant response [11] plus the double-resonance peak.

One interesting feature of the response function, seen in experiments on correlated materials [2,3], and seen in theoretical calculations of the nonresonant response [11,12], is that at low energy there is an isosbestic point, where the response function is essentially independent of temperature at a particular frequency $\Omega \approx U/2$. Below that frequency the response decreases as T is lowered, and above it increases. The isosbestic behavior must survive in the Loudon-Fleury regime, because the isosbestic point is at low energy, and the low-energy response is negligible in the resonant and mixed contributions. But what happens when $\omega_i \approx U$? Here we expect interesting effects to occur, because the incident photon energy is the right size to cause transitions from the lower to upper Hubbard bands of the correlated insulator. Indeed, we find interesting results in this regime (Fig. 2). At low temperature ($T < 0.7$), a symmetry-dependent isosbestic point appears at a transferred frequency of 0.7–0.9 and is seen in all channels at low enough T. Hence the inclusion of resonant and mixed terms provides theoretical support for the generic presence of a low-temperature isosbestic point in all correlated systems, in full agreement with light-scattering measurements on Kondo and mixed-valent compounds [2,3].

Finally, we present results of what the resonant profile of the scattering looks like by fixing the transferred frequency and varying the incident photon energy. We expect that there will be a resonant peak in the response, and indeed this is so, although in some cases the double resonance overwhelms the presence of the peak. Note that in our theoretical results, in addition to the expected resonance that occurs when the incident photon frequency is close to the transferred frequency, another resonance occurs, where the low-energy peak is strongly enhanced when $\omega_i \approx U$ and is qualitatively similar to what is seen with the two-magnon resonance [4,5] in high-

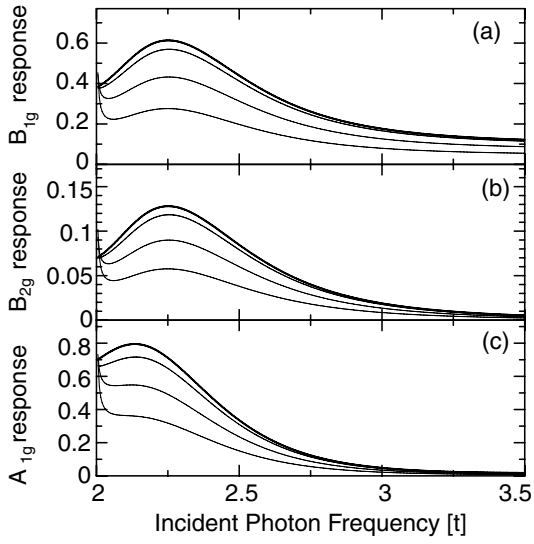

FIG. 3. Raman response function for $U = 2$ and $\Omega = 2$ for different channels at $T = 1$, $T = 0.5$, $T = 0.2$, and $T = 0.05$. The temperature decreases as the lines are made thicker.

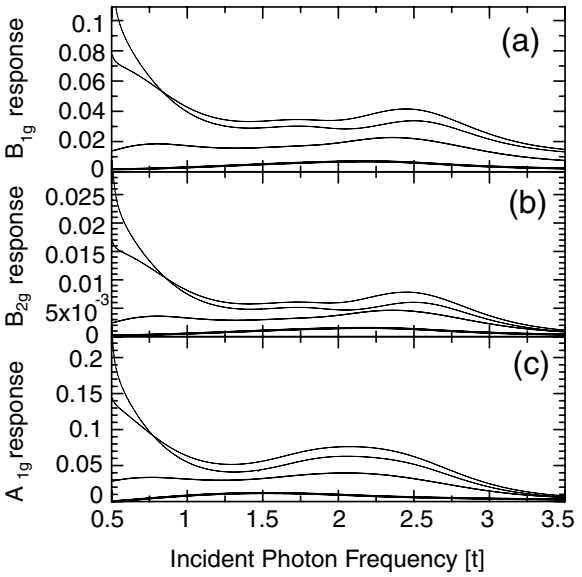

FIG. 4. Raman response function for $U = 2$ and $\Omega = 0.5$ for different channels at $T = 1$, $T = 0.5$, $T = 0.2$, and $T = 0.05$. The temperature decreases as the lines are made thicker.

temperature superconductors, even if the physics behind the joint resonance effect is different here. We show this regime in Figs. 3 ($\Omega = 2.0$) and 4 ($\Omega = 0.5$). In Fig. 3 we see a moderately broad peak centered at ω_i 10–20% higher than U. The enhancement of the charge-transfer peak in this regime can easily be an order of magnitude over the nonresonant response. In Fig. 4, we see a similar resonant feature when the incident photon frequency is slightly larger than $\Omega = 0.5$ (arising from the double-resonance effect and at too low a photon energy to be experimentally observable in most materials), but a second less prominent series of broad peaks occurs when $\omega_i \approx U$ indicating that the low-energy and charge-transfer peaks are resonating together when $\omega_i \approx U$ (the width of this broad peak, on the order of t^*, is similar to the 1 eV width seen in the high-temperature superconductors). Hence the joint resonance effect observed for the two-magnon response in the high-temperature superconductors [4,5] might be observable in many other correlated insulators [2,3,6], that do not have magnons, via this alternative strongly correlated process.

Finally we comment on finite-dimensional effects and the relevance of our calculations to real materials. In finite dimensions more diagrams enter into the irreducible vertex function, but we have seen by comparing different Raman response functions, that many features remain similar even when additional diagrams are present in one channel (A_{1g}) and not another (B_{1g}). Hence we expect that the qualitative features we observe here will emerge in finite dimensions as well.

In conclusion, we have shown a number of interesting resonant features in theoretical calculations of electronic Raman scattering. These features include the double resonance, the resonant enhancement of nonresonant peaks, the appearance of isosbestic points, and the joint resonance of low-energy and charge-transfer peaks when $\omega_i \approx U$. It will be interesting to see whether these predictions can be seen in a variety of correlated insulators, as conjectured.

We wish to acknowledge the U.S. Civilian Research and Development Foundation through grant no. UP2-2436-LV-02. J. K. F. also acknowledges the National Science Foundation through grant no. DMR-0210717, and T. P. D. acknowledges funding from NSERC, PREA, and the A. v. Humboldt Foundation.

[1] A. Kotani and S. Shin, Rev. Mod. Phys. **73**, 203 (2001).
[2] P. Nyhus, S. L. Cooper, and Z. Fisk, Phys. Rev. B **51**, 15626 (1995).
[3] P. Nyhus *et al.*, Phys. Rev. B **52**, R14308 (1995); Phys. Rev. B **55**, 12488 (1997).
[4] K. B. Lyons *et al.*, Phys. Rev. Lett. **60**, 732 (1988); S. Sugai, S. Shamoto, and M. Sato, Phys. Rev. B **38**, 6436 (1988); P. E. Sulewsky *et al.*, Phys. Rev. B **41**, 225 (1990); R. Liu *et al.*, J. Phys. Chem. Solids **54**, 1347 (1993).
[5] G. Blumberg *et al.*, Phys. Rev. B **53**, 11930 (1996).
[6] H. L. Liu *et al.*, Phys. Rev. B **60**, R6980 (1999).
[7] P. M. Platzman and E. D. Isaacs, Phys. Rev. B **57**, 11107 (1998).
[8] B. S. Shastry and B. I. Shraiman, Phys. Rev. Lett. **65**, 1068 (1990); Int. J. Mod. Phys. B **5**, 365 (1991).
[9] P. A. Fleury and R. Loudon, Phys. Rev. **166**, 514 (1968).
[10] A. V. Chubukov and D. M. Frenkel, Phys. Rev. B **52**, 9760 (1995); Phys. Rev. Lett. **74**, 3057 (1995); D. K. Morr and A. V. Chubukov, Phys. Rev. B **56**, 9134 (1997).
[11] J. K. Freericks and T. P. Devereaux, Condens. Matter Phys. **4**, 149 (2001); Phys. Rev. B **64**, 125110 (2001).
[12] J. K. Freericks *et al.*, Phys. Rev. B **64**, 233114 (2001); J. K. Freericks *et al.*, Phys. Rev. B **67**, 155102 (2003).
[13] We have not been able to prove that the three and four-particle vertices do not enter for the resonant Raman scattering, but a strong-coupling perturbative analysis indicates that this is so to lowest order.
[14] A. M. Shvaika, Physica C (Amsterdam) **341-348**, 177 (2000); J. K. Freericks and P. Miller, Phys. Rev. B **62**, 10022 (2000); A. M. Shvaika, J. Phys. Stud. **5**, 349 (2001).
[15] L. M. Falicov and J. C. Kimball, Phys. Rev. Lett. **22**, 997 (1969).
[16] W. Metzner and D. Vollhardt, Phys. Rev. Lett. **62**, 324 (1989).
[17] U. Brandt and C. Mielsch, Z. Phys. B **75**, 365 (1989); **79**, 295 (1990).
[18] V. Zlatić *et al.*, Philos. Mag. B **81**, 143 (2001); J. K. Freericks and V. Zlatić, Rev. Mod. Phys. **75**, 1333 (2003).
[19] T. P. Devereaux *et al.*, Phys. Rev. Lett. **90**, 067402 (2003); Phys. Rev. B **68**, 075105 (2003).
[20] Model independence does not hold for metallic systems for nonresonant scattering [11,12] and thus we would expect different resonant signatures in the metallic phases of different models.